Published in final edited form as:
J Biomech. 2015 February 26; 48(4): 627–635. doi:10.1016/j.jbiomech.2014.12.051.

Intracellular forces during guided cell growth on micropatterns using FRET measurement

Kevin Suffoletto[1], **Nannan Ye**[1], **Fanjie Meng**[2], **Deepika Verma**[1], and **Susan Z. Hua**[1,2,*]

[1]Department of Mechanical and Aerospace Engineering, Biophysics, SUNY-Buffalo, Buffalo, New York 14260, USA

[2]Department of Physiology, Biophysics, SUNY-Buffalo, Buffalo, New York 14260, USA

Abstract

Interaction of cells with extracellular matrix (ECM) regulates cell shape, differentiation and polarity. This effect has been widely observed in cells grown on substrates with various patterned features, stiffness and surface chemistry. It has been postulated that mechanical confinement of cells by the substrate causes a redistribution of tension in cytoskeletal proteins resulting in cytoskeletal reorganization through force sensitive pathways. However, the mechanisms for force transduction during reorganization remain unclear. In this study, using FRET based force sensors we have measured tension in an actin cross-linking protein, α-actinin, and followed reorganization of actin cytoskeleton in real time in HEK cells grown on patterned substrates. We show that the patterned substrates cause a redistribution of tension in α-actinin that coincides with cytoskeleton reorganization. Higher tension was observed in portions of cells where they form bridges across inhibited regions of the patterned substrates; the attachment to the substrate is found to release tension. Real time measurements of α-actinin tension and F-actin arrangement show that an increase in tension coincides with formation of F-actin bundles at the cell periphery during cell-spreading across inhibited regions, suggesting that mechanical forces stimulate cytoskeleton enhancement. Rho-ROCK inhibitor (Y27632) causes reduction in actinin tension followed by retraction of bridged regions. Our results demonstrate that changes in cell shape and expansion over patterned surfaces is a force sensitive process that requires actomyosin contractile force involving Rho-ROCK pathway.

Keywords

protein forces; micro-patterning; cell adhesion; cytoskeleton reorganization; actomyosin

*Corresponding author information: 340 Jarvis Hall, SUNY-Buffalo, Buffalo, NY, 14260. zhua@buffalo.edu.

Conflict of interest statement: None of the authors have any financial or personal conflict of interest with regard to this study.

Introduction

The mechanical interaction and linkages between a cell and the substrate play a critical role in cell morphology, motility, proliferation, and growth (DuFort et al., 2011; Thery et al., 2006b; Xia et al., 2008). In adherent cells, the mechanical forces from the substrate can be transmitted to cell body via integrins that link ECM proteins with the cytoskeleton at focal adhesions (Discher et al., 2005; Geiger et al., 2001; Ladoux et al., 2008). Through this link, the geometry and rigidity of the substrate imposes mechanical constraints on the cytoskeleton, thus regulating cell processes (Hahn and Schwartz, 2009; Ingber, 2003).

The modification of cell shape by patterned substrates has been widely observed, where cells are selectively attached to patterns made of adhesive proteins using surface patterning techniques (Karuri et al., 2008; Lehnert et al., 2004). For example, cells grown on triangular patterns have an overall triangular shape; such cells developed thick bundles of stress fibers along the non-adhesive edges suggesting a reinforcement of the cytoskeleton in response to the geometrical constraints (Thery et al., 2006a; Wang et al., 2007). Similarly, cells grown on narrow stripes align themselves along the orientation of the stripes. Substrate geometry also affects cell polarity and provides guidance for cell expansion and migration direction (Jiang et al., 2005; Kumar et al., 2007). Although these results provide the end-point of cell morphology under a mechanical constraint, only recently the role of internal mechanical forces in cell remodeling has been explored, namely, the process leading to the end point (DuFort et al., 2011; Grashoff et al., 2010; Maruthamuthu et al., 2011).

The cytoskeleton of adherent cells is prestressed by internally generated forces and this stress is equilibrated by the resistive forces due to the substrate. Imposing physical boundaries to the cells via a patterned substrate can alter the distribution of internal forces, thereby activating force sensitive cellular processes responsible for cell remodeling. It has been reported that a higher contractile force is required for cells to form a bridge across patterned regions where the adhesion is inhibited (Rossier et al., 2010). Similarly, application of an external mechanical force by cyclically stretching the substrate or by fluid shear stress can also modify the rate of actin turnover and arrangement of the actin stress fibers (Tzima, 2006; Verma et al., 2012). Since both applied mechanical stimuli and geometrical constraints alter the distribution of actin filaments, it is logical to predict that these cellular processes are facilitated by changes in forces in cytoskeletal proteins. Although such a viewpoint has been generally accepted, the internal forces leading to the structural modification in a patterned cell remains to be determined.

Previously, various traction force microscopy techniques have been used to measure forces exerted by a cell onto the substrate (Tambe et al., 2011; Wang and Lin, 2007). Tan *et al.* (Tan et al., 2003) have used arrays of microfabricated polydimethylsiloxane (PDMS) pillars that are compliant to the cellular traction. Another sensing method utilizes fluorescent nanobeads as markers that are imbedded in flexible substrates (Sabass et al., 2008; Schwarz et al., 2003). To make organized adhesions, fluorescently labeled protein dots were directly printed on the surface of the flexible substrates (Polio et al., 2012). These methods measure the net force arising from the sum total of all the actin filaments that are linked to the adhesion. Since the number of filaments is difficult to quantify and it also varies with time,

the forces in linking proteins cannot be measured with TFM. Recently, we have developed a series of FRET based force sensors that can be genetically inserted in specific cytoskeleton cross-linking proteins that allows us to measure the changes in tension induced by external or internal forces (Meng and Sachs, 2011; Meng et al., 2008). Similar techniques were later developed by others (Borghi et al., 2012; Grashoff et al., 2010). The FRET sensor provides the true measure of stresses in the linking proteins. Moreover, the FRET-based technique enables non-contact measurements of intracellular tension, thereby opening the possibility to independently vary the mechanical properties of the substrate.

In this study we have measured tension in cytoskeletal crosslinking protein α-actinin, using FRET based force sensors in Human Embryonic Kidney (HEK) cells. Cells were subjected to a variety of well defined mechanical constraints imposed by patterned substrates. Results show that the substrate features cause a redistribution of tension in α-actinin and reorganization of the actin cytoskeleton. We show that an increase in tension is required for the formation of peripheral actin bundles where cells form bridges across inhibited regions of the patterned substrate suggesting that changes in cytoskeletal tension are involved in cytoskeleton reorganization; this process is mediated by Myosin-II contractility.

Materials and methods

Micro-contact printing

A standard microprinting method was used to pattern the extracellular matrix protein fibronectin on cover slide substrates. Briefly, a PDMS stamp was created using SU-8 mold following previously developed processes (Wang et al., 2010). The stamp was exposed to 50 μg/ml fibronectin (an adhesive protein) in water for 1 hr to coat the proteins onto its surface. Separately, a glass substrate was silanized with 5% dichlorodimethylsilane in 1,2-dichlorobenzene solution for 10 sec, followed by exposure to UV light for 10 min, which modifies the wettability of the silanized surface. The fibronectin coated PDMS stamp was then brought into physical contact with the glass substrate, printing the fibronectin pattern onto the substrate. To prevent non-selective cell adhesion on non-patterned regions, the patterned glass slide was subsequently immersed into a blocking reagent (0.2 % Pluronics F-127) for 1 hr.

Actinin-sstFRET sensor

The FRET based force probe sstFRET (spectrin-repeat stress sensitive FRET), consists of a pair of fluorophores, Cerulean (donor) and Venus (acceptor), that are linked by spectrin repeat domain (linker); the sensor construction has been described previously (Meng and Sachs, 2011; Meng et al., 2008). The sensor cassette is inserted into the middle of the host protein, α-actinin, at amino acid position 300, and is termed as ‘actinin-sstFRET’. Under an axial force the distance between the donor and acceptor is extended, leading to a decrease in FRET efficiency, and thus, an overall decrease in the measured FRET acceptor/donor (A/D) ratio. Previously, the probes has been carefully characterized so that the chimeric constructs behave as endogenous proteins (e.g., α-actinin) and the labeling does not interfere with physiological functions of the cell (Meng and Sachs, 2011). The sensitivity of the sensor has also previously been determined *in vitro* by attaching the sensor to a deformable substrate

and stretching the substrate, and *in vivo* in many cell types including HEK, MDCK, and fibroblast (Meng et al., 2008). A control probe has been constructed by attaching the sstFRET cassette to the C-terminal of α-actinin with one end attached to α-actinin and another end being free-floating, and is termed 'actinin-C-sstFRET'. We have previously shown experimentally that actinin-C-sstFRET probes are insensitive to forces in actinin (Meng and Sachs, 2011).

FRET imaging and image analysis

Fluorescence images were obtained using an inverted microscope (Axiovert 200M, Zeiss) with a 63× oil immersion objective and an EM-CCD camera (ImagEM C9100-13, Hamamatsu). Donor and acceptor channels were acquired simultaneously using a dual-view optical system (Optical Insights, USA). The excitation filter set includes a bandpass filter (CFP: 436 ± 20 nm) and a dichroic mirror (455 DCLP); the emission filter set includes two emission filters (480±30 nm and 535±40 nm) for CFP and YFP channels respectively, and a dichroic mirror (505DCXR). Time-lapse movies were obtained using Zeiss software (AxioVision, Ziess). The images from CFP and YFP channels were aligned and the ratio of YFP/CFP was calculated using Image-J (from NIH). The bleed-through from CFP to YFP was calibrated prior to experiments and was subtracted during image processing (Meng et al., 2008; Xia and Liu, 2001). The FRET ratio (YFP/CFP) is shown in a 16 color map, where warm colors illustrate a higher FRET ratio, indicating lower tension; cool colors indicate a lower FRET ratio, i.e., a higher tension. For time dependent measurements, the image acquisitions were started at 2 hrs after seeding. Each measurement was conducted using a new cell culture. To obtain reliable intracellular force distribution, images were taken after cells had fully spread on the patterned area in ∼3 hrs. For statistical analysis, the lowest tension state (highest FRET ratio) from each cell was averaged over the entire cell population, and the averaged value was used as a reference for the lowest tension state for all cells. This enables us to minimize FRET signal variations from cell to cell. The FRET ratio in each subcellular region was measured for each cell and then averaged over multiple cells. Statistical data is expressed as means ± standard error of the means (s.e.m.), and was analyzed using Paired sample t-test. Values of $p < 0.05$ were considered statistically significant.

Cell culture and transfection

HEK293 cells (ATCC) were cultured in Dulbecco's Modified Eagle Medium (DMEM) containing fetal bovine serum and 1% penicillin and streptomycin. Cells were transfected 24 hrs before the experiments with actinin-sstFRET or actinin-C-sstFRET using Effectene Transfection Reagent (Qiagen, CA) following manufacturer's specifications. Transfection efficiency was ∼40%. The transfected cells were trypsinized and seeded onto the patterned substrates and cultured at 37 °C for 2 hrs. Unattached cells were gently washed away using PBS before imaging.

Results

To understand the role of cytoskeletal forces in cell spreading and morphology, we expressed the FRET based force sensor, actinin-sstFRET, in patterned cells, and observed

changes in actinin stress during cell spreading (Fig. 1a). The sensor is located in the middle of α-actinin, as shown in Fig. 1b. In the relaxed state FRET is maximal since the donor and acceptor are closer. Under a stretching force, the distance between the two fluorophores increases and FRET ratio decreases (Fig. 1b). For control, the force insensitive variant of FRET probe, actinin-C-sstFRET, was used (Fig. 1c) (Meng and Sachs, 2011). By expressing actinin-sstFRET in cells and subsequently staining F-actin with phalloidin, we have previously shown that actinin-sstFRET and F-actin co-localize along the actin filaments in cells (Rahimzadeh et al., 2011). Thus, actinin-sstFRET (CFP channel) probes can also be used as labels for F-actin to monitor the cytoskeleton reorganization in live cells.

We first examined the shape and distribution of the actin cytoskeleton in cells grown on various patterns using actinin-sstFRET. The patterns consisted of parallel stripes (6 μm wide and 10 μm apart), T-shape (6 μm wide and 30 μm long along both directions), and hexagon (30 μm between any two parallel edges of the hexagon), as shown in Fig. 2, left column. These patterns are designed to host a single cell and provide geometrical constraints upon directional expansion (Stripes), forced bridging across non-adhesive areas (T-shape), and uniform growth as a control (Hexagon). The spatial arrangement of actin cytoskeleton was monitored using actinin-sstFRET (CFP channel) in live cells (Fig. 2, middle column), and results show that cells are able to adhere, spread, and reorganize their cytoskeleton on the patterned substrates within 2 hrs. This effect of the pattern geometry on actin cytoskeleton and cell morphology can be observed for periods up to 12 hrs. Following live cell imaging, cells were fixed and stained with fluorescein-phalloidin to obtain F-actin structure at high resolution, as shown in Fig. 2, right column.

Cells respond to substrate confinement through reorganization of the cytoskeleton and changes in their shape. On narrow stripes, cells expanded along the length and ballooned out along the stripe width forcing the cell to partially float over the inhibited surface at the central region of the cell. On T-shape pattern, cells spread along all three arms and bridge across the inhibited regions to form a triangular shape. A higher density of stress fibers were formed at the edge of such bridged regions, consistent with previous observations in other cell types (Thery et al., 2006a). In contrast, cells on hexagon patterns show a distribution of fibers within the patterned regions. Cells frequently exhibited lamellipodia extrusions beyond the patterned regions, and retracted back towards the patterned region due to the non-adhesive condition (see supplementary material, Fig. S1). A similar cell activity has been observed in all patterns. Cells spread through a process involving increase of contractile forces, initiation of new adhesions, and enlargement of focal adhesion size (Giannone et al., 2007). When cells reached the boundaries of the pattern, a new adhesion is not able to form even though the lamellipodium can reach out of the patterned region. Such a limit may send a feedback signal to modulate the myosin contractility, and further affect downstream cytoskeletal reorganization that is initiated by focal adhesion proteins.

To obtain a statistical representation of the internal force distribution on patterned cells, we measured the tension in actinin using actinin-sstFRET sensors when the cells had fully spread onto the patterns. The typical fluorescent images (CFP channel) and the corresponding FRET ratio of a cell stabilized on the patterns are shown in Fig. 3a-c and Fig. 3d-f, respectively. Cells demonstrated a distinctive distribution of tension on each pattern.

On rectangular patterns, cells show a higher tension (lower FRET ratio) in the central region that often extends and bulges outside the patterned area, and lower tension at the elongated regions of the cell attached to the pattern (Fig. 3a,d). This result suggests that the tension is reduced due to cell attachment. On T-shaped patterns, cells spread out along all three ends to form a triangle (Fig. 3b). Higher tension is seen at the bridged regions where the adhesion is prohibited, Fig. 3e; lower tension was observed at the attached regions (Fig. 3b,e). In contrast, cells on hexagonal patterns demonstrate a random distribution of tension when the cell spreads and adheres to the patterned area (Fig. 3c,f). The statistics of FRET ratio in each region are shown in Fig. 3g-i, for stripes (n=9), T-shape (n=15), and hexagons (n=9), respectively. Statistical analysis shows that tension at the bridged regions of the cell on a T-shaped pattern (left gray bar in Fig. 3h) is significantly higher than at the attached regions (left red bar in Fig. 3h). This suggests that higher actinin tension is required for a cell across an inhibited region while enhanced forces are not necessary to maintain the mature adhesion regions within the pattern. As a control, actinin-C-sstFRET expressing cells were also grown on the patterns, and the FRET ratio in actinin-C-sstFRET was measured using the same protocol. Actinin-C-sstFRET expressing cells showed a consistently higher FRET ratio (lower tension) in all regions (stripes, n=16; T-shape, n=15; hexagon, n=15). This is expected since actinin-C-sstFRET probe cannot be stressed by the cells. Additionally, larger variation in tension among different areas was normally seen at the beginning of cell attachment, followed by a reduction in average tension during the extended attachment on the patterns. A higher actinin tension is probably required only during spreading and migration.

To examine the role of tension in cell remodeling, we analyzed the time dependent FRET ratio in bridged and central regions during the cell spreading process on T-shaped patterns. It was found that actinin tension increases in the bridged regions and this increase in tension is accompanied by the formation of F-actin bundles across the inhibited surface. A time sequence of actinin-FRET images (CFP channel) and corresponding FRET ratio from a representative cell is shown in Fig. 4a,b, respectively, during the cell spreading. A concave edge was observed initially between two adhesive arms (blue arrow, in Fig. 4a, t=0), and the connection expanded outwards resulting in thick bundles of actin filaments at the suspended edges (yellow arrow, in Fig. 4a, t=30 min). The FRET ratio decreases in these regions, indicating that an increase in tension is associated with cell expansion over the inhibited region (Fig. 4b). In contrast, although the formation of F-actin bundles in the bridged regions is also shown in actinin-C-sstFRET expressing cell (Fig. 4c), the FRET ratio remains unchanged in this cell (Fig. 4d). Time dependence of FRET ratio from selected regions is plotted in Fig. 4e,f for actinin-sstFRET and actinin-C-sstFRET, respectively, showing that a drastic increase in tension occurs between 0 and 11 min for bridge B2 and between 0 and 6 min for bridge B1, respectively, followed by an approach to a steady tension level in the actinin-sstFRET expressing cell (Fig. 4e). Change in tension in the bridged regions before and after cell spreading was analyzed from multiple cells (n =15), and the statistics is shown in Fig. 4g, left column. A frame-by-frame comparison between actin reorganization and change in regional tension further reveals that the maximal stress changes occur prior to the development of F-actin bundles at the edge of the bridged region that appears to start at ∼18 min in Fig. 4a; it suggests that mechanical forces could be

responsible for the assembly and enhancement of F-actin seen in the bridged regions. The increase in tension is also observed in the attached edges but to a lesser extent, resulting in a relatively lower tension at the steady state (Fig. 4e).

Since RhoA and ROCK are known to regulate adhesion dynamics, actin orientation and organization, we tested whether Rho-regulated myosin-II contraction force plays a role in guided cell growth on the patterns. Cells on T-shaped patterns were exposed to ROCK inhibitor (Y27632) after they were fully spread and no longer exhibited morphological changes. Time sequence of actin cytoskeletal structure in typical actinin-sstFRET and actinin-C-FRET expressing cells are shown in Fig. 5a and b, respectively. It shows that blocking Rho-ROCK with 10 μM Y27632 causes a retraction of cell from bridged regions towards the adhesive regions within 30 min (Fig. 5a), and this retraction coincides with a reduction in tension (increase in FRET ratio) in bridged regions, as measured using actinin-sstFRET (Fig. 5c). This reduction in tension is also seen in the attached region but to a lesser extent because lower tension is present in those regions before the application of the drug. The forces from different regions approach the same level in ∼30 min in the presence of the drug (Fig. 5c). Similar structural changes were observed in cells expressing actinin-C-sstFRET, however, there was no noticeable change in FRET ratio in all of the selected regions (Fig. 5d). The drug effect was found to be reversible. Following the washout, the bridged regions regained higher tension (low FRET) accompanied by extension of cell edges to re-form a triangular shape. This behavior was consistent over repeated experiments. The statistics for cells before and after drug treatment is shown in Fig. 5e (red). In contrast, FRET ratio in actinin-C-sstFRET is consistently higher in all regions (green, Fig. 5e). This suggests that regions spanning across the inhibited areas are highly stressed and myosin-II mediated contraction is accountable for the measured tension.

Discussion

Adherent cells experience a variety of extra-cellular forces through their contacts with the substrate, which affect their stress state and subsequent activities. A growing body of evidence supports that cells recognize and respond to variations in substrate geometry via mechanosensitive pathways that trigger the assembly and disassembly of actin cytoskeleton. In this work, forces in α-actinin have been measured in real-time using FRET, in cells on patterned substrates. The FRET measurement takes the ratio of YFP and CFP fluorescence intensities, making the measurement independent of the protein density; therefore, it is a true measure of the stress in the cross-linking protein (α-actinin). Our results show that the increase in actinin tension only occurs when cells spread on the patterned substrate, which results in the formation of actin bundles across inhibited regions.

Since we measure the mean value of fluorescence from hundreds to thousands of proteins (within resolution of optical microscopy), the tension in linking proteins is a reasonable indicator of the local tension in actin cytoskeleton. For instance, although α-actinin can crosslink actin at all orientations in an actin bundle, histograms have shown that the crosslinks occur at preferential angles, namely, at 0, 60, 90, 120, and 180 degrees (Hampton et al., 2007). While ∼25% of the crosslinks are oriented between 80 and 100 degrees (showing a ladder like configuration), more than 75% are oriented at ≤ 60 degrees or ≥ 120

degrees. Thus, a uniaxial tension along actin filaments will cause an increase in actinin tension in our measurements. Moreover, a differential movement or shear between adjacent filaments will also cause an increase in tension in actinin. We have also previously shown that actinin-sstFRET and F-actin co-localize along the actin cytoskeleton in cells. Therefore, the FRET probes can be used as label for F-actin to monitor actin translocation, as well as a quantitative method of measuring forces within the cytoskeletal structure in real time.

Using our method, we have examined cell behavior on three patterns, T-shape, narrow stripes and hexagons, all hosting a single cell. Our results show that higher tension is associated with bridging regions that cross over the inhibited areas, specifically, the bridges across extended arms on a T-shaped pattern and the central regions that bulge out of the adhesive surface of stripes (Fig. 3). This result differs from TFM measurements that show greatest traction force occurring at cell periphery. The FRET sensor measures tension in individual protein (α-actinin), whereas TFM measures the net force arising from the sum total of all the actin filaments that are linked to the adhesion. Since the number of actin filaments varies with time, the forces in linking proteins for each filament cannot be quantified by TFM. For instance, FRET sensors report forces in the range of 2-10 pN, the tension in actinin (Meng and Sachs, 2011); typical traction forces are on the order of 10-60 nN (Tan et al., 2003). Our results show that force in actinin increases prior to and during cell spread-out across the bridging regions, suggesting mechanical forces are responsible for the formation of thick bundles of actin filaments.

The increased force in actinin during cell locomotion is dynamically linked with focal adhesion development. We have recently shown that an increase in tension in α-actinin at the focal adhesion occurs during adhesion growth in migrating (non-patterned) cells (Ye et al., 2014). When the adhesion reaches its stable size, tension is reduced to a level comparable with the surrounding areas (Ye et al., 2014). Similar changes in contractile force have been obtained using TFM (Stricker et al., 2011). On the pattern, actinin tension increases when the cell bridges across the non-adhering regions. When a cell is limited by the pattern, the adhesions on the patterned surface reached a saturated size resulting in reduced tension and a more stable force distribution. Our results provide evidence that increase in cytoskeletal tension is required only during spreading and migration. Interestingly, these cells demonstrated an active reach-out lamellipodium associated with variation in force at the pattern boundaries. There is no net increase in tension at the protrusions when adhesion is prohibited by the pattern. This result also provides evidence that a cell utilizes the substrate geometry as one of the signaling pathways to modulate the tension in proteins, resulting in assembly or disassembly of cytoskeleton.

To determine the participation of Rho-ROCK pathways in the observed actin enhancement at the bridged regions, we blocked the pathway using ROCK inhibitor Y27632. The drug effectively reduced the contraction forces in 5 min, followed by a reduction in actin density at the bridged regions. This effect is reversible, and recovery of both forces and actin density is observed in 30 min after washout (data not shown). These results support the argument that bridge formation in cells grown on patterns is mediated by Rho-ROCK pathways (Rossier et al., 2010). Our results also suggest that a shear between the adjacent actin

filaments may occur due to myosin generated sliding, resulting in a higher tension in α-actinin in the bridged or bulged regions.

In conclusion, using FRET based force sensors we have demonstrated a novel method for measuring forces in proteins during cell's adaptation on patterned substrates. Results show an increase in actinin tension when cells extend over the non-adhesive regions, resulting in formation of thick actin bundles. This force generation and cytoskeleton enhancement requires the activation of Rho-ROCK pathways.

Supplementary Material

Refer to Web version on PubMed Central for supplementary material.

Acknowledgments

This work was supported by National Science Foundation Grant CMMI-0825707 and National Institutes of Health Grant NS085517.

References

Borghi N, Sorokina M, Shcherbakova OG, Weis WI, Pruitt BL, Nelson WJ, Dunn AR. E-cadherin is under constitutive actomyosin-generated tension that is increased at cell-cell contacts upon externally applied stretch. Proceedings of the National Academy of Sciences of the United States of America. 2012; 109:12568–12573. [PubMed: 22802638]

Discher DE, Janmey P, Wang YL. Tissue cells feel and respond to the stiffness of their substrate. Science (New York, NY. 2005; 310:1139–1143.

DuFort CC, Paszek MJ, Weaver VM. Balancing forces: architectural control of mechanotransduction. Nature reviews. 2011; 12:308–319.

Geiger B, Bershadsky A, Pankov R, Yamada KM. Transmembrane crosstalk between the extracellular matrix--cytoskeleton crosstalk. Nature reviews. 2001; 2:793–805.

Giannone G, Dubin-Thaler BJ, Rossier O, Cai Y, Chaga O, Jiang G, Beaver W, Dobereiner HG, Freund Y, Borisy G, Sheetz MP. Lamellipodial actin mechanically links myosin activity with adhesion-site formation. Cell. 2007; 128:561–575. [PubMed: 17289574]

Grashoff C, Hoffman BD, Brenner MD, Zhou R, Parsons M, Yang MT, McLean MA, Sligar SG, Chen CS, Ha T, Schwartz MA. Measuring mechanical tension across vinculin reveals regulation of focal adhesion dynamics. Nature. 2010; 466:263–266. [PubMed: 20613844]

Hahn C, Schwartz MA. Mechanotransduction in vascular physiology and atherogenesis. Nature reviews. 2009; 10:53–62.

Hampton CM, Taylor DW, Taylor KA. Novel structures for alpha-actinin:F-actin interactions and their implications for actin-membrane attachment and tension sensing in the cytoskeleton. Journal of molecular biology. 2007; 368:92–104. [PubMed: 17331538]

Ingber DE. Mechanosensation through integrins: cells act locally but think globally. Proceedings of the National Academy of Sciences of the United States of America. 2003; 100:1472–1474. [PubMed: 12578965]

Jiang X, Bruzewicz DA, Wong AP, Piel M, Whitesides GM. Directing cell migration with asymmetric micropatterns. Proceedings of the National Academy of Sciences of the United States of America. 2005; 102:975–978. [PubMed: 15653772]

Karuri NW, Nealey PF, Murphy CJ, Albrecht RM. Structural organization of the cytoskeleton in SV40 human corneal epithelial cells cultured on nano- and microscale grooves. Scanning. 2008; 30:405–413. [PubMed: 18626907]

Kumar G, Ho CC, Co CC. Guiding cell migration using one-way micropattern arrays. Advanced Materials. 2007; 19:1084–1090.

Ladoux B, Ghibaudo M, Saez A, Trichet L, Xayaphoummine A, Browaeys J, Silberzan P, Buguin A. Traction forces and rigidity sensing regulate cell functions. Soft Matter. 2008; 4:1836–1843.

Lehnert D, Wehrle-Haller B, David C, Weiland U, Ballestrem C, Imhof BA, Bastmeyer M. Cell behaviour on micropatterned substrata: limits of extracellular matrix geometry for spreading and adhesion. Journal of cell science. 2004; 117:41–52. [PubMed: 14657272]

Maruthamuthu V, Sabass B, Schwarz US, Gardel ML. Cell-ECM traction force modulates endogenous tension at cell-cell contacts. Proceedings of the National Academy of Sciences of the United States of America. 2011; 108:4708–4713. [PubMed: 21383129]

Meng F, Sachs F. Visualizing dynamic cytoplasmic forces with a compliance-matched FRET sensor. Journal of cell science. 2011; 124:261–269. [PubMed: 21172803]

Meng F, Suchyna TM, Sachs F. A fluorescence energy transfer-based mechanical stress sensor for specific proteins in situ. The FEBS journal. 2008; 275:3072–3087. [PubMed: 18479457]

Polio SR, Rothenberg KE, Stamenovic D, Smith ML. A micropatterning and image processing approach to simplify measurement of cellular traction forces. Acta biomaterialia. 2012; 8:82–88. [PubMed: 21884832]

Rahimzadeh J, Meng F, Sachs F, Wang J, Verma D, Hua SZ. Real-time observation of flow-induced cytoskeletal stress in living cells. Am J Physiol Cell Physiol. 2011; 301:C646–652. [PubMed: 21653900]

Rossier OM, Gauthier N, Biais N, Vonnegut W, Fardin MA, Avigan P, Heller ER, Mathur A, Ghassemi S, Koeckert MS, Hone JC, Sheetz MP. Force generated by actomyosin contraction builds bridges between adhesive contacts. The EMBO journal. 2010; 29:1055–1068. [PubMed: 20150894]

Sabass B, Gardel ML, Waterman CM, Schwarz US. High resolution traction force microscopy based on experimental and computational advances. Biophysical journal. 2008; 94:207–220. [PubMed: 17827246]

Schwarz US, Balaban NQ, Riveline D, Addadi L, Bershadsky A, Safran SA, Geiger B. Measurement of cellular forces at focal adhesions using elastic micro-patterned substrates. Mat Sci Eng C-Bio S. 2003; 23:387–394.

Stricker J, Aratyn-Schaus Y, Oakes PW, Gardel ML. Spatiotemporal constraints on the force-dependent growth of focal adhesions. Biophysical journal. 2011; 100:2883–2893. [PubMed: 21689521]

Tambe DT, Hardin CC, Angelini TE, Rajendran K, Park CY, Serra-Picamal X, Zhou EH, Zaman MH, Butler JP, Weitz DA, Fredberg JJ, Trepat X. Collective cell guidance by cooperative intercellular forces. Nature materials. 2011; 10:469–475.

Tan JL, Tien J, Pirone DM, Gray DS, Bhadriraju K, Chen CS. Cells lying on a bed of microneedles: an approach to isolate mechanical force. Proceedings of the National Academy of Sciences of the United States of America. 2003; 100:1484–1489. [PubMed: 12552122]

Thery M, Pepin A, Dressaire E, Chen Y, Bornens M. Cell distribution of stress fibres in response to the geometry of the adhesive environment. Cell Motil Cytoskeleton. 2006a; 63:341–355. [PubMed: 16550544]

Thery M, Racine V, Piel M, Pepin A, Dimitrov A, Chen Y, Sibarita JB, Bornens M. Anisotropy of cell adhesive microenvironment governs cell internal organization and orientation of polarity. Proceedings of the National Academy of Sciences of the United States of America. 2006b; 103:19771–19776. [PubMed: 17179050]

Tzima E. Role of small GTPases in endothelial cytoskeletal dynamics and the shear stress response. Circulation research. 2006; 98:176–185. [PubMed: 16456110]

Verma D, Ye N, Meng F, Sachs F, Rahimzadeh J, Hua SZ. Interplay between cytoskeletal stresses and cell adaptation under chronic flow. PloS one. 2012

Wang J, Heo J, Hua SZ. Spatially resolved shear distribution in microfluidic chip for studying force transduction mechanisms in cells. Lab on a chip. 2010; 10:235–239. [PubMed: 20066252]

Wang JH, Lin JS. Cell traction force and measurement methods. Biomech Model Mechanobiol. 2007; 6:361–371. [PubMed: 17203315]

Wang YL, Mader CC, Hinchcliffe EH. Probing cell shape regulation with patterned substratum: requirement of myosin II-mediated contractility. Soft Matter. 2007; 3:357–363.

Xia N, Thodeti CK, Hunt TP, Xu Q, Ho M, Whitesides GM, Westervelt R, Ingber DE. Directional control of cell motility through focal adhesion positioning and spatial control of Rac activation. Faseb J. 2008; 22:1649–1659. [PubMed: 18180334]

Xia Z, Liu Y. Reliable and global measurement of fluorescence resonance energy transfer using fluorescence microscopes. Biophysical journal. 2001; 81:2395–2402. [PubMed: 11566809]

Ye N, Verma D, Meng F, Davidson MW, Suffoletto K, Hua SZ. Direct observation of α-actinin tension and recruitment at focal adhesions during contact growth. Experimental cell research. 2014

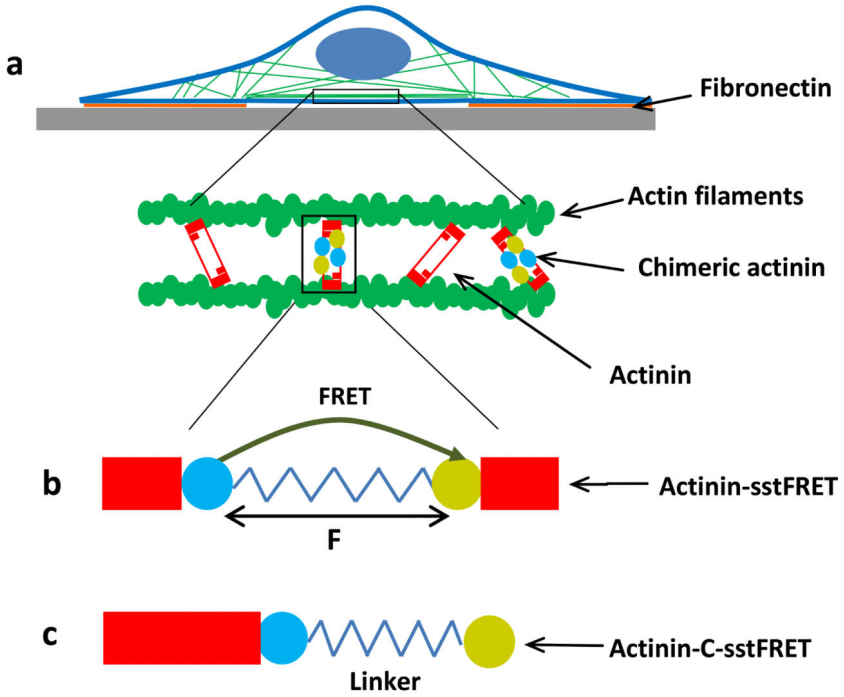

Figure 1.

Schematic of FRET probe construction and their distribution in a patterned cell. **a**: FRET probes are inserted in α-actinin that cross-link actin filaments. **b**: Construction of actinin-sstFRET. Stress sensor cassette, consisting of Cerulean, donor, Venus, acceptor and a linker, that is located at amino acid 300, close to the middle of actinin. Resting sensor shows higher FRET. Under axial force (F) the distance between donor and acceptor is extended leading to lower FRET (higher tension). **c:** Construction of force-free variant probe, actinin-C-sstFRET. The FRET pair is linked to the C-terminal of actinin, thus, is not able to sense actinin tension.

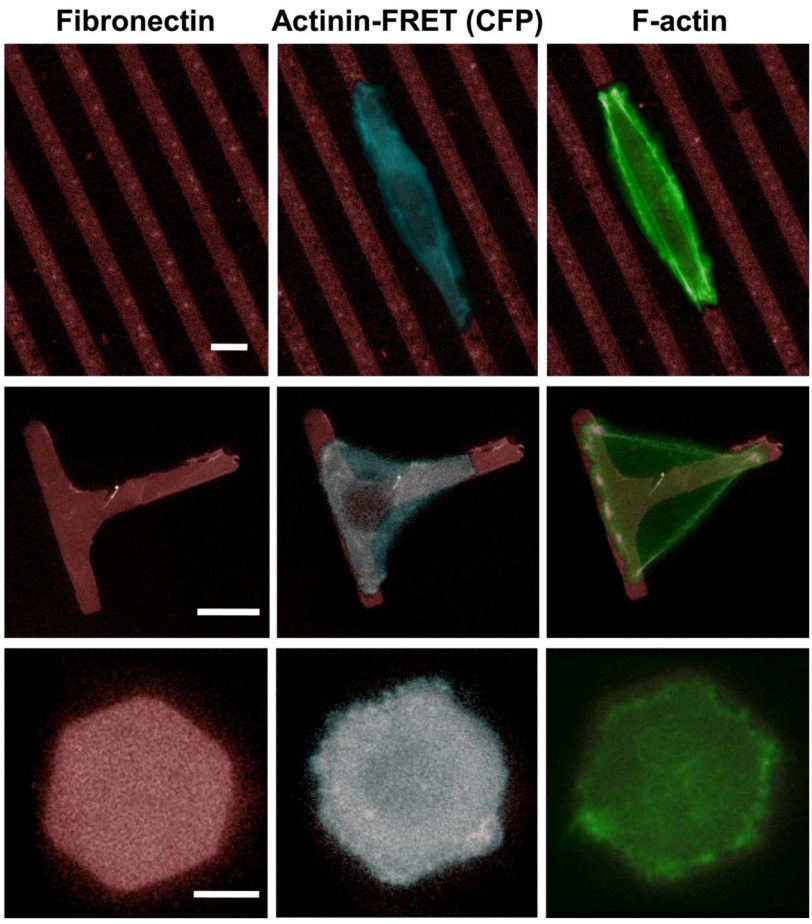

Figure 2.

Images of cells expressing actinin-sstFRET on patterned substrates. Left panel: Geometry of three patterns, parallel stripes, T-shape and hexagon. Middle panel: Fluorescence images of actinin-sstFRET (CFP channel, blue) in live cells on patterned fibronection (red). The images were taken 2 hours after seeding. Right panel: Immuno-stained actin (green) after cells were stabilized on the patterns, showing the formation of actin bundles at the cell periphery when it expands to the restricted regions (middle region on stripes and the bridges on T-shape pattern). Scale bars represent 10 μm.

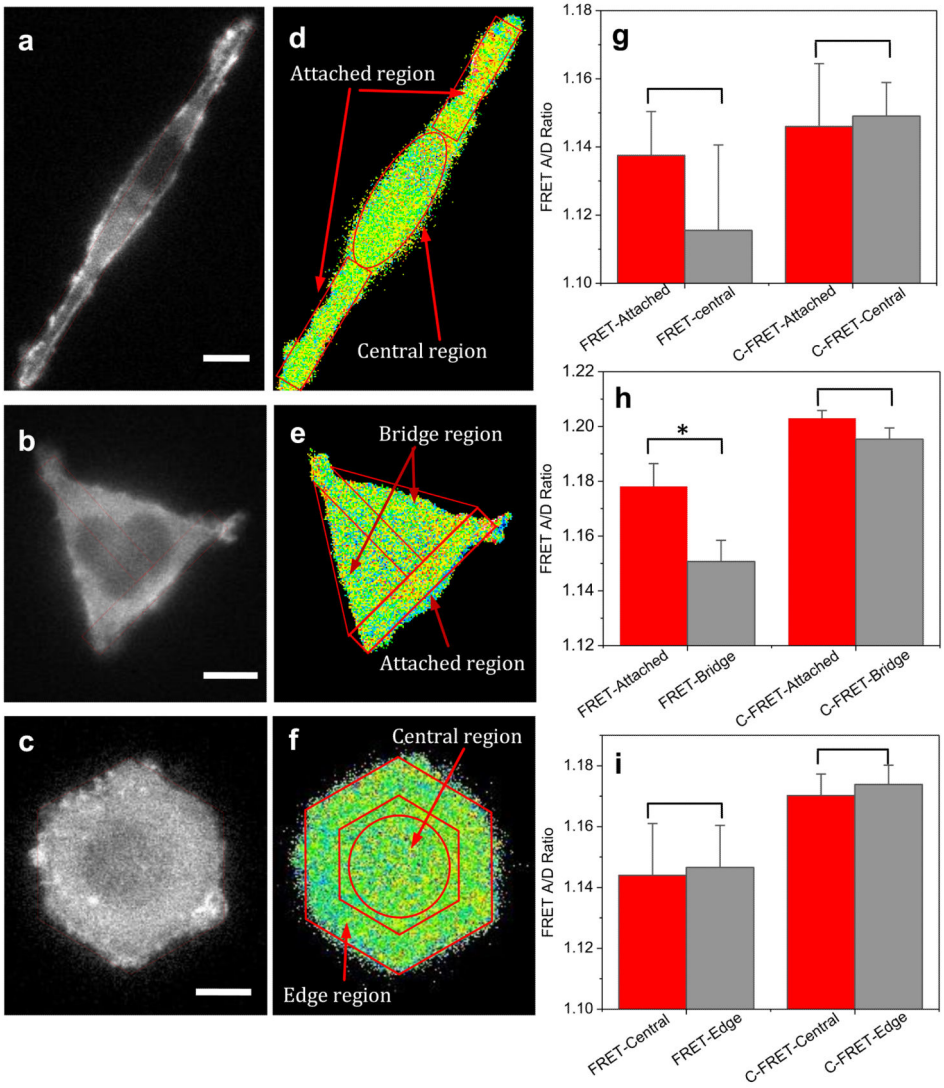

Figure 3.

Distribution of tension in actinin in cells grown on various patterns. **a-c:** Fluorescent images of actinin-sstFRET (CFP channel) of a HEK cell on stripes **(a)**, T-shape **(b)**, and hexagon **(c)**. Red dashed lines show the outlines of patterned region. **d-f**: Corresponding FRET ratio in each cell, showing the distribution of tension in actinin. Lower FRET ratio (blue color) indicates higher tension, while higher FRET ratio indicates lower tension. The images were taken ∼3 hrs after cell seeding on the patterns. **g-i**: Statistics of FRET ratio in each region marked in **(d-f)** measured using actinin-sstFRET (left group) and actinin-C-sstFRET (right group), respectively. FRET ratio (actinin-sstFRET) from non-adhering regions were compared with attached regions for stripes (n=9, $p = 0.28$), T-shape (n=15, $*p = 0.0048$), and hexagons (n=9, $p = 0.80$). * indicates the difference between two groups is statistically significant. FRET ratio in actinin-C-sstFRET from the corresponding regions were also compared for stripes (n=16, $p = 0.95$), T-shape (n=15, $p = 0.74$), and hexagons (n=15, $p = 0.74$). Scale bars represent 10 μm.

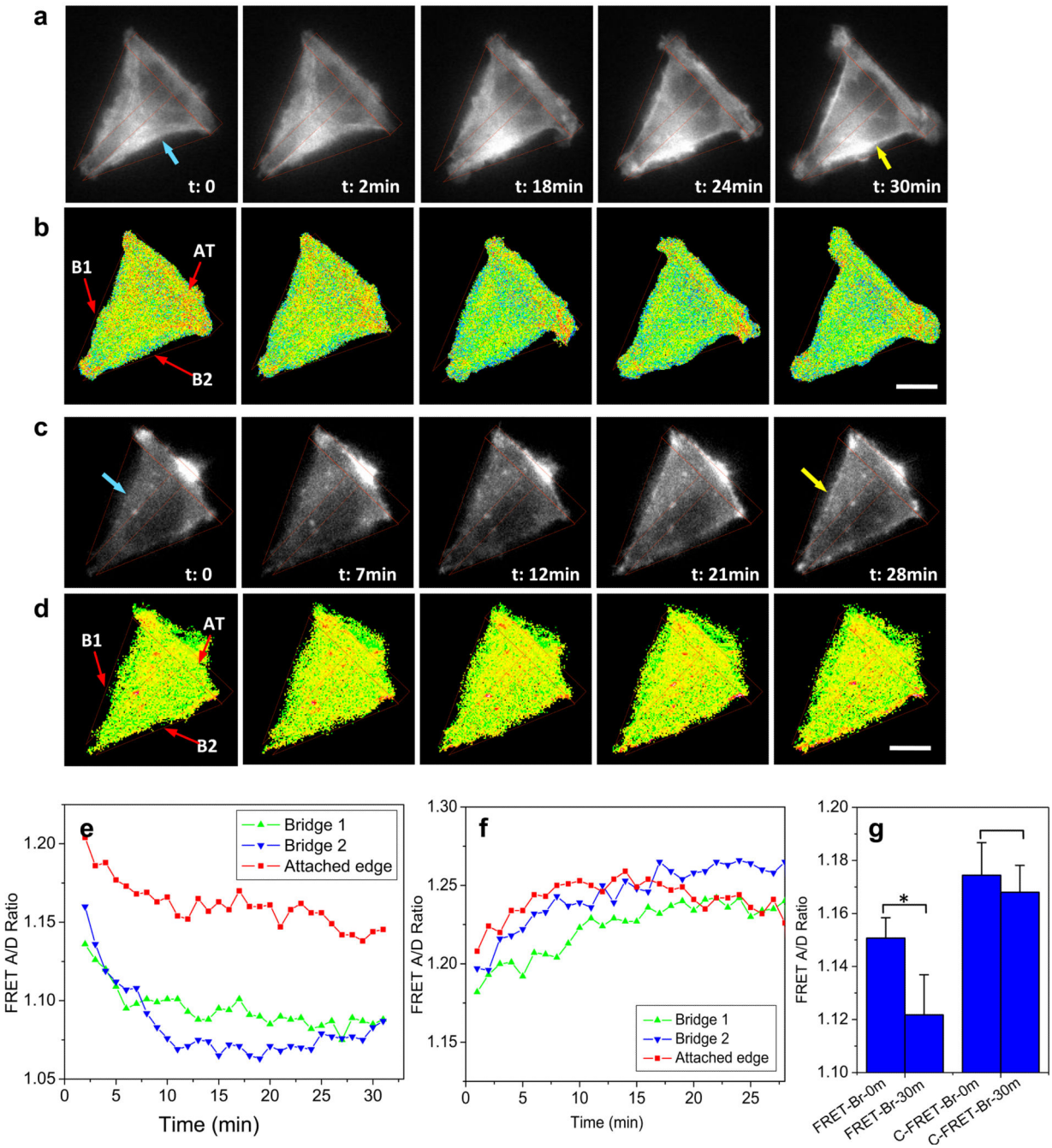

Figure 4.

Time-dependent changes in actinin tension and corresponding cytoskeleton reorganization in cells grown on T-shape pattern. **a,b**: Live cell fluorescent images of actinin-sstFRET (CFP channel) and corresponding FRET ratio, showing correlated changes of actin structure and tension during cell spreading on the T-shape pattern. **c,d**: Same recording for actinin-C-sstFRET. **e,f**: Time-dependent changes in tension in selected regions indicated in (**b** and **d**), bridges (B1 and B2) and attached edge (AT), using actinin-sstFRET and actinin-C-sstFRET probes, respectively. **g**: Change in actinin tension in bridged regions before and after 30 min

of spreading. The data is averaged from multiple cells (n=15, *p = 0.013) and the control cells (n = 5, p = 0.4). Scale bars represent 10 μm.

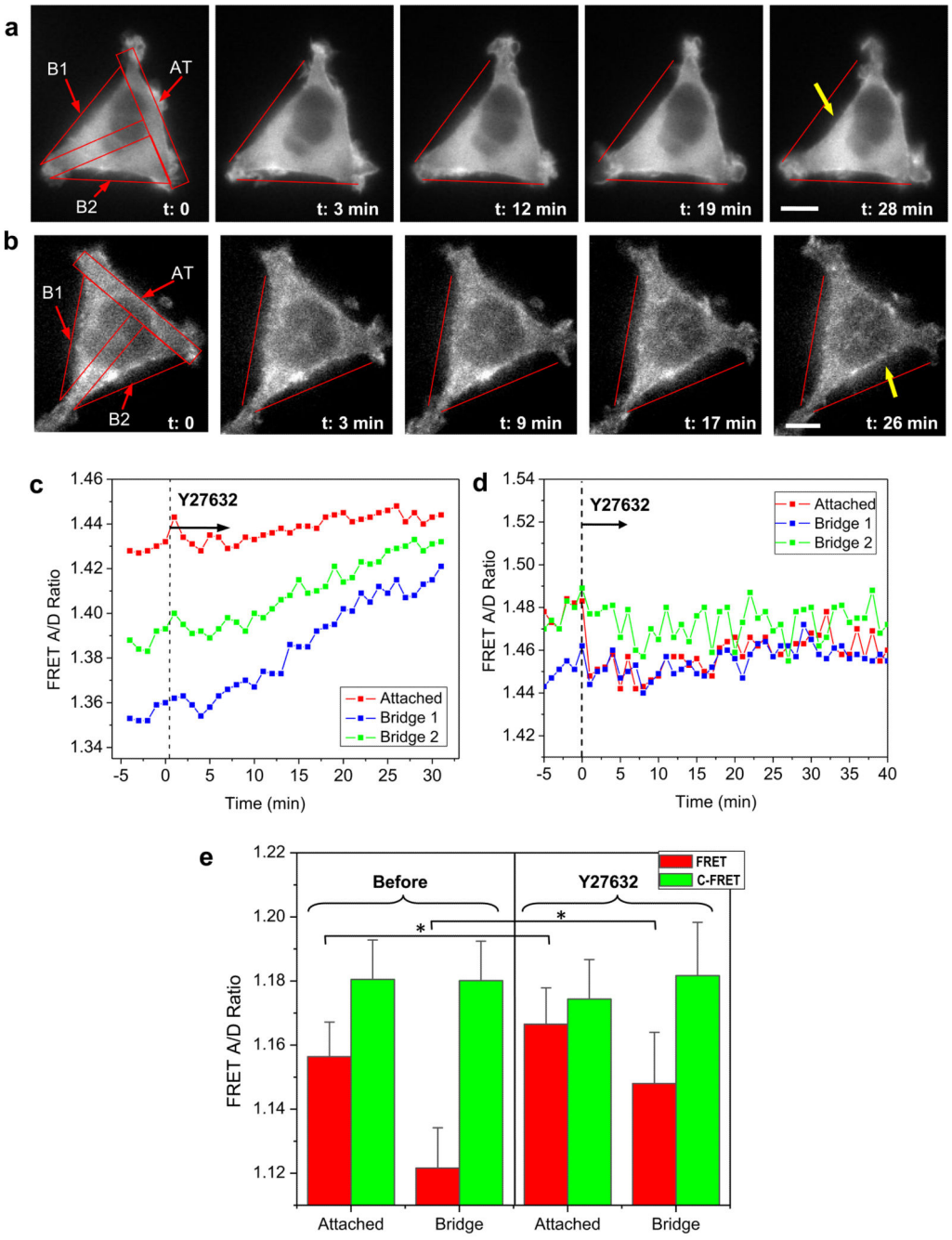

Figure 5.

Effect of Rho-ROCK inhibitor on pattern-induced actinin tension and changes in cell shape. **a,b**: Time series of fluorescent images of actinin-sstFRET and actinin-C-sstFRET before and during application of Y27632. After cells spread on T-shape pattern, they were exposed to Y27632 (10 μM) at time zero, indicated by dashed line in (**c** and **d**). Scale bars represent 10 μm. **c:** Time plot of tension in attached region (AT) (red) and bridged regions (B1, B2) (blue, green) from **(a)**, showing Rho inhibitor causes reduction of tension, and this coincides with a retraction of cell edges at bridged regions (indicated by yellow arrow in (**a**)). **d:** Same

measurement using control probes (acinin-C-sstFRET) from **(b),** showing the drug does not induce significant change in tension in different regions. **e:** Statistics of FRET ratio in actinin-sstFRET in attached region and bridged regions, before and 30 min after application of Y27632 (red bars, attached n = 9, **p* = 0.032; bridge n = 9, **p* = 0.034). Similar measurement using actinin-C-sstFRET (green bars, attached n = 5, *p* = 0.96; bridge n = 5, *p* = 0.48).